Borrelia burgdorferi periplasmic flagella have both skeletal and motility functions

Mohammed Abdul Motaleb*, Linda Corum*, James L. Bono†, Abdallah F. Elias†, Patricia Rosa†, D. Scott Samuels‡, and Nyles W. Charon*§

*Department of Microbiology and Immunology, Health Sciences Center, West Virginia University, Box 9177, Morgantown, WV 26506; †Laboratory of Human Bacterial Pathogenesis, Rocky Mountain Laboratories, National Institute of Allergy and Infectious Diseases, National Institutes of Health, Hamilton, MT 59840; and ‡Division of Biological Sciences, University of Montana, Missoula, MT 59812

Edited by Allan Campbell, Stanford University, Stanford, CA, and approved August 1, 2000 (received for review May 15, 2000)

Bacterial shape usually is dictated by the peptidoglycan layer of the cell wall. In this paper, we show that the morphology of the Lyme disease spirochete *Borrelia burgdorferi* is the result of a complex interaction between the cell cylinder and the internal periplasmic flagella. *B. burgdorferi* has a bundle of 7–11 helically shaped periplasmic flagella attached at each end of the cell cylinder and has a flat-wave cell morphology. Backward moving, propagating waves enable these bacteria to swim in both low viscosity media and highly viscous gel-like media. Using targeted mutagenesis, we inactivated the gene encoding the major periplasmic flagellar filament protein FlaB. The resulting *flaB* mutants not only were nonmotile, but were rod-shaped. Western blot analysis indicated that FlaB was no longer synthesized, and electron microscopy revealed that the mutants were completely deficient in periplasmic flagella. Wild-type cells poisoned with the protonophore carbonyl cyanide-*m*-chlorophenylhydrazone retained their flat-wave morphology, indicating that the periplasmic flagella do not need to be energized for the cell to maintain this shape. Our results indicate that the periplasmic flagella of *B. burgdorferi* have a skeletal function. These organelles dynamically interact with the rod-shaped cell cylinder to enable the cell to swim, and to confer in part its flat-wave morphology.

spirochete | Lyme disease | allelic exchange | morphology

Spirochetes have a unique position among the bacteria. These motile bacteria are one of the few bacterial phyla that can be identified by both 16S ribosomal RNA sequence analysis and morphology (1). Outermost is a membrane sheath, and within this sheath are the cell cylinder and periplasmic flagella. A given periplasmic flagellum is attached subterminally at only one end of the cell cylinder, and it resides within the periplasmic space (2). Depending on the species, the cell morphology is either a helix, a flat wave, or an irregularly shaped helix (2–4). The size of the spirochete, the number of periplasmic flagella attached at each end, and whether the filaments overlap at the center of the cell varies from species to species (2, 5). This phylum contains many medically important bacteria including *Treponema pallidum* (syphilis), several *Borrelia* species (relapsing fever), *Borrelia burgdorferi* (Lyme disease), *Leptospira interrogans* (leptospirosis), *Brachyspira* sp. (human diarrheal disease, swine dysentery), and oral treponemes associated with periodontal disease (5–8).

The periplasmic flagella of spirochetes have been characterized in detail. Genetic evidence, including targeted mutagenesis studies in *Treponema denticola* and *Brachyspira hyodysenteriae*, have shown that these organelles are directly involved in motility (9, 10) (C. Li and N.W.C., unpublished observations). By analyzing protruding periplasmic flagella from certain motility mutants of *T. phagedenis*, and from stationary-phase cells of several spirochete species, these organelles have been shown to rotate in a manner similar to that of flagella of other bacteria (4, 11). An analysis of the genome sequences of both *B. burgdorferi* and *T. pallidum* indicates that practically all of the genes required for motility and chemotaxis are present in these species (12, 13). In fact, some spirochetal motility genes are so similar to those of *Escherichia coli* and *Salmonella enterica* serovar Typhimurium that their expression in these bacteria result in negative complementation effects on flagella synthesis and motility. A likely explanation for this negative complementation is that the spirochetal motility proteins compete and interfere with their counterparts with respect to assembly of flagellar components (14, 15).

Recent results with *B. burgdorferi* indicate that the morphology of these spirochetes is likely to be influenced by the presence of the periplasmic flagella. These spirochetes are quite large relative to other bacteria, with a diameter of 0.33 μm and a length of 10–20 μm (16). They have a flat-wave morphology with a wavelength of 2.83 μm, and a peak-to-peak amplitude of 0.78 μm (4, 16). Attached at each end are 7–11 periplasmic flagella that overlap in the center of the cell (7). These periplasmic flagella consist of the major filament protein FlaB and a minor filament protein FlaA (17). Sadziene *et al.* (18) isolated a spontaneously occurring, nonmotile mutant (HB19Fla$^-$). HB19Fla$^-$ lacked periplasmic flagella and both FlaA and FlaB proteins (17, 18). It initially was described as helical but somewhat straighter than the parental strain (18). Subsequent light and high-voltage electron microscopy analyses revealed that HB19Fla$^-$ had a long, rod-shaped morphology (4, 16). The helical morphology observed by Sadziene *et al.* was most likely the consequence of cells occasionally growing in chains and wrapping around each other in a right-handed sense (4). The result that single HB19Fla$^-$ cells were rod-shaped led to formulation of the hypothesis that the periplasmic flagella influenced the entire shape of the cell. Moreover, a model of *B. burgdorferi* motility was proposed based on this hypothesis (4, 16) (see ref. 19 for recent review). A significant concern with this analysis is that the site and nature of the mutation (or mutations) in HB19Fla$^-$ is unknown; analysis of many of the flagellar genes of HB19Fla$^-$, including the flagellar filament *flaB* gene, failed to identify the mutation in HB19Fla$^-$ (18, 20, 21). Thus, the mutant could be rod-shaped for reasons other than the lack of periplasmic flagella.

The genetic analysis of spirochetes, including *B. burgdorferi*, has been hindered by the lack of an efficient method for targeted mutagenesis. Thus, drawing conclusions on a molecular level regarding gene function has been difficult. Recently, an efficient allelic exchange mutagenesis method was developed for *B. burgdorferi*. This method uses a kanamycin-resistant cassette derived from *E. coli* Tn*903* fused to either of two *B. burgdorferi*

This paper was submitted directly (Track II) to the PNAS office.

Abbreviation: CCCP, carbonyl cyanide-*m*-chlorophenylhydrazone.

§To whom reprint requests should be addressed. E-mail: ncharon@hsc.wvu.edu.

The publication costs of this article were defrayed in part by page charge payment. This article must therefore be hereby marked "*advertisement*" in accordance with 18 U.S.C. §1734 solely to indicate this fact.

Article published online before print: *Proc. Natl. Acad. Sci. USA*, 10.1073/pnas.200221797. Article and publication date are at www.pnas.org/cgi/doi/10.1073/pnas.200221797

periplasmic flagellar promoters (22). Using this method, we show by allelic exchange mutagenesis that inactivation of *flaB* results in cells that lack periplasmic flagella and are nonmotile. Because these mutant cells have a markedly altered morphology, we conclude that the periplasmic flagella also have a skeletal function dictating, at least in part, the flat-wave morphology associated with intact cells.

Materials and Methods

Bacterial Strains and Growth Conditions. High-passage culture-attenuated *B. burgdorferi* senso stricto strain B31 has been described (23). Cells were grown in liquid at 32°C and on plates at 34°C in BSK-II medium (23, 24). Solid medium and agar overlay were prepared by using 0.66% agarose (23). Liquid medium and agar plates were incubated in an atmosphere of 3% carbon dioxide. Swarm plate assays were carried out by using 0.35% agarose; approximately 5×10^5 washed cells in 5 μl were spotted onto plates containing BSK-II medium diluted 1:10 in Dulbecco's PBS without divalent cations. To test for the inhibition of motility by the protonophore carbonyl cyanide-*m*-chlorophenylhydrazone (CCCP), 5 ml of logarithmic phase cells was centrifuged at 1,000 $\times$ *g* at room temperature. The pellet was gently resuspended in 1 ml of 10 mM PBS, pH 7.0, containing 5 mM glucose also at room temperature (25). After CCCP was added to a final concentration of 20 μM, cell motility was observed over the next 30 min. As a positive control, we also assayed *S. enterica* serovar Typhimurium strain SJW 1103 under similar conditions (obtained from R. Macnab, Yale University, New Haven, CT).

Construction of Plasmid pGFbKAN. The *flaB* gene and flanking DNA were first amplified by PCR with primers P1 and P2 from chromosomal DNA of strain B31, and the product obtained was cloned into plasmid pGEM-T Easy (Promega) to yield pGFb (Fig. 1). We used the 1.3-kb *flgB*-kanamycin resistance cassette (*kan*) to inactivate *flaB* (22). *kan* was inserted at the *Age*I site of *flaB* in pGFb to yield plasmid pGFbKAN. Restriction mapping indicated that the direction of transcription of *kan* was opposite to that of *flaB*.

Allelic Exchange Mutagenesis. Unless otherwise stated, all procedures for genetic manipulations were carried out according to standard methods (26). PCR was done with *Pfu* or *Taq* DNA polymerase (Promega). The primers (5′-3′) used are the following (see Fig. 1): P1, AGTTCTTCCTGCATTTCTCC; P2, GCAATCCTTAAAGGAGGGCA; P3, GCTGCTACAACC TCATCTG; P4, AGCTTTCTAGTGGGTACA; P5, AGCCAT-TATCACCACCAGAG; P6, TCCCATGACCGTGAAAT-CCA; KAN1, GGGAAACGTCGAGGCCGCG; KAN2, GAATGAGCTAGCGCCGTCCCG; KAN3, ACCGGTTAAT-ACCCGAGCTTCAAGGAAG; KAN4, ACCGGTGGC-GAATGAGCTTGCGCCGTCC. Preparation of competent *B. burgdorferi*, electroporation, and plating of transformants were done as described (23). Approximately 4 μg of input DNA was used for electroporation. Electroporated cells were mixed with molten agar after 20 h of incubation and grown in BSK-II medium in the presence of 350 μg/ml kanamycin (22, 23).

Gel Electrophoresis and Western Blot Analysis. SDS/PAGE and Western blotting with the ECL detection method (Amersham Pharmacia) were carried out as reported (17). Monoclonal antibody H9724 to *B. burgdorferi* FlaB was generously provided by A. Barbour (University of California, Irvine) (27). Cell lysates and purified periplasmic flagella were prepared as described (17).

Light and Electron Microscopy. Cell motility and morphology were analyzed by using phase optics with a Zeiss Axioskop 2 microscope. A DAGE 72X MTI video camera, a JVC SR-S-365U video recorder, and a Sony UP-910 Videographic printer were used for image analysis (3). Imbedding and fixation of *B. burgdorferi* cells for electron microscopic analysis have been described (16). Sections were viewed with a JEOL 1020 microscope at an accelerating voltage of 80 kV.

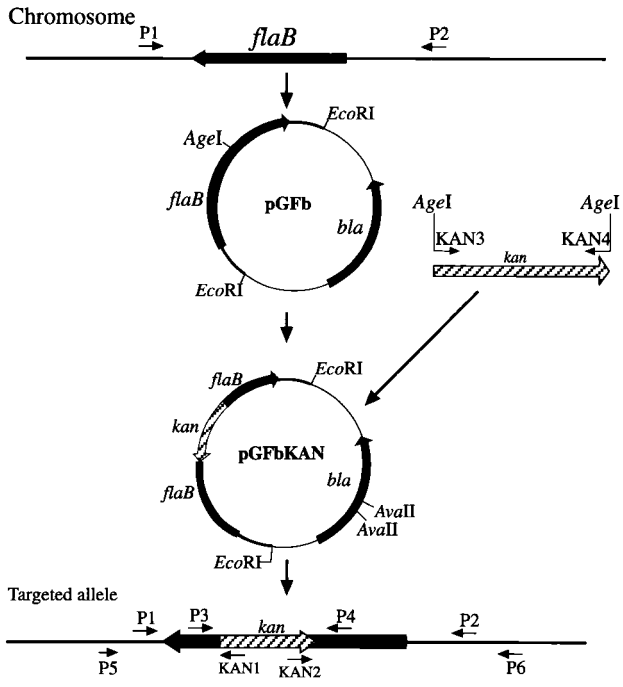

Fig. 1. Construction of plasmid vehicle pGFbKAN used to inactivate *flaB*. pGFb was derived from both the pGEM-T Easy vector and amplified *flaB* plus flanking DNA by using primers P1 and P2. The *kan* cassette was amplified with *Age*I-containing restriction sites with primers KAN3 and KAN4 and inserted into *Age*I site of pGFb to yield plasmid pGFbKAN. After digestion with *Eco*RI and *Ava*II, the purified linear fragment containing *flaBkan* was used for allelic exchange. Wide arrows indicate direction of transcription. P represents PCR primers. *bla* is the β-lactamase gene. Plasmids are not drawn to scale.

Results

Construction of *flaB* Mutant. We used recombinant DNA techniques to insert *kan* into the gene that encodes the major filament protein *flaB*. *flaB* maps at position 147652–148659 on the linear chromosome of *B. burgdorferi*; it is transcribed as a monocistronic mRNA toward the left telomere (13, 18, 28). To optimize chances of obtaining recombinants, greater than 1.2 kb of *B. burgdorferi* DNA flanked each side of the cassette (29). Insertion vehicle plasmid pGFbKAN was digested with *Eco*RI and *Ava*II (see Fig. 1) to inactivate the vector-encoded ampicillin resistance gene and prevent its transfer into *B. burgdorferi*. The gel-purified 4.7-kb *flaB-kan* linear fragment was used for electroporation. In contrast to wild-type colonies that appear after 10–12 days incubation, transformant colonies took approximately 18 days to be detected and were quite small (<0.1 mm). Eleven such colonies were picked and grown in BSK-II containing kanamycin.

We used PCR methodology to determine whether allelic exchange at *flaB* occurred as predicted (Figs. 1 and 2). Amplification of the DNA obtained from the clones with primers P3 and P4 indicated that *kan* inserted within the *flaB* gene in 10 of 11 mutants isolated. As shown in Fig. 2*a*, the PCR product obtained from the representative mutant MC-1 was 2.1 kb, which is similar to the amplified product from plasmid pGFbKAN. This product was larger than that obtained from the wild type, which

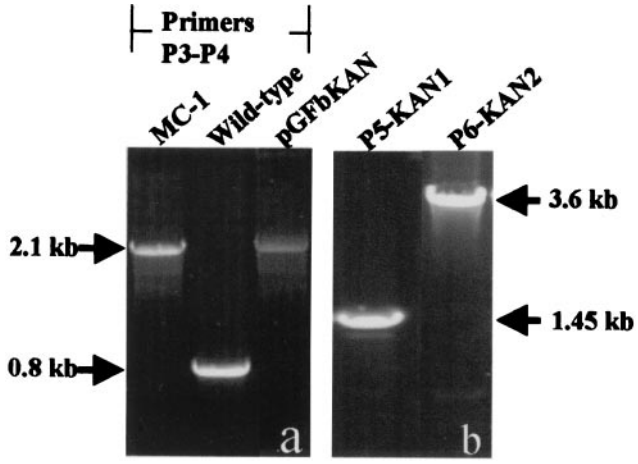

Fig. 2. Confirmation of *kan* insertion into *flaB*. PCR analysis of wild-type and resultant kanamycin-resistant mutant MC-1 using primer pair P3-P4 (*a*) and junction PCR products using the *kan*-specific primers and primers P5 and P6 (*b*). The location of the primers are shown in Fig. 1.

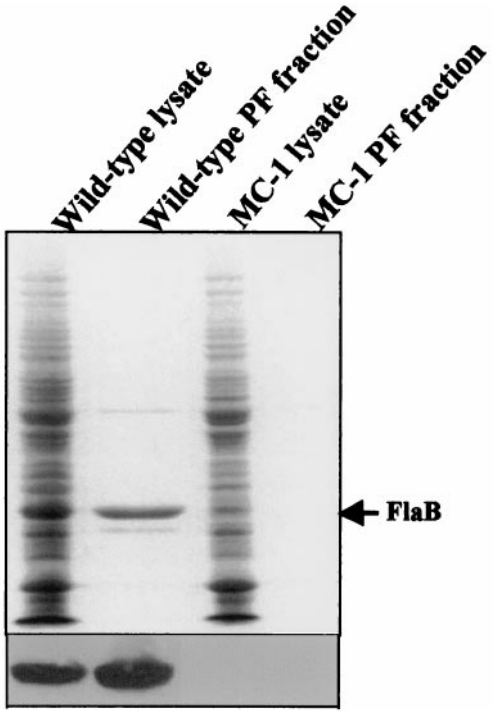

Fig. 3. Detection of FlaB synthesis. SDS/PAGE (*Upper*) and Western blot analysis (*Lower*) of mutant MC-1 and the wild type using FlaB monoclonal antibody H9724. Purified periplasmic flagella is abbreviated as PF.

was 800 bp. As a further test for the *kan* insertion occurring on the bacterial chromosome in MC-1, we amplified the DNA with primer pairs P5-KAN1 and P6-KAN2. Primers P5 and P6 flank *flaB* outside of the region that initially was used for cloning, and primers KAN1 and KAN2 bind within the *kan* cassette (Fig. 1). MC-1 yielded amplified junction products consistent with the *kan* cassette inserting into the chromosomally located *flaB* (Fig. 2*b*). Southern blot analysis also substantiated that MC-1 contained the kanamycin insert in *flaB* (not shown).

Flagellar Synthesis in the MC-1 *flaB* Mutant. MC-1 was characterized in detail, but it had identical phenotypic characteristics common to all 10 mutants with the same PCR patterns. Because FlaB is readily identified in *B. burgdorferi* cell lysates by SDS/PAGE, Coomassie blue staining revealed that MC-1 was deficient in FlaB synthesis (Fig. 3 *Upper*). Western blot analysis indicated that both the cell lysate and the purified periplasmic flagella from the wild type was recognized by a FlaB monoclonal antibody (Fig. 3 *Lower*). However, no FlaB was detected in the MC-1 mutant cell lysate or mock-purified periplasmic flagella. These results indicate that FlaB synthesis is inhibited in the MC-1 mutant.

Because *flaB* encodes the major filament protein, we assayed for periplasmic flagella by electron microscopy. Periplasmic flagella were readily evident in wild-type cells (Fig. 4 *a* and *b*). Mutant MC-1 completely lacked periplasmic flagella (Fig. 4 *c* and *d*). No filament structures were observed in any cells examined. These results suggest that mutants unable to synthesize FlaB are also deficient in periplasmic flagella.

Altered Motility and Morphology of *flaB* Mutant. We tested whether the *flaB* mutation resulted in a loss of motility and an altered cell morphology. Examination of mutant MC-1 by light microscopy indicated that it was completely nonmotile, whereas the wild type was fully motile. In addition, mutant MC-1 failed to swarm on soft agarose plates, whereas the wild type spread quite readily (Fig. 5). These results indicate that inactivation of *flaB* results in cells that are nonmotile.

We compared the morphology of MC-1 to the wild type. Light microscopic examination indicated that, whereas the wild-type cells had a flat-wave morphology, mutant MC-1 was rod-shaped (Fig. 6). In addition, MC-1 grew as long chains with incomplete division planes. The rod-shaped morphology of MC-1 was clearly seen in thin sections of mutant MC-1 by electron microscopy (Fig. 4*d*). Thin sections of wild-type cells revealed a pattern consistent with a flat-wave morphology (Fig. 4*b*). The rod-shaped morphology and motility defect of MC-1 were stable characteristics, as cells grown several generations without kanamycin were still nonmotile and rod-shaped. The results taken together indicate that inactivation of *flaB* is responsible for the loss in motility and altered morphology.

Relationship Between Energy Transduction and Cell Morphology. We examined the relationship between motility and the flat-wave morphology of *B. burgdorferi*. Two possible explanations are readily apparent. First, perhaps only motile cells with actively rotating periplasmic flagella have a flat-wave morphology. Along these lines, the anterior spiral wave found in translating *Leptospiraceae* is associated with active flagellar rotation; cells at rest have hooked-shaped ends (30, 31). This hypothesis predicts that if the periplasmic flagella of *B. burgdorferi* stop rotating, the cell would become rod-shaped. An alternative hypothesis states that the periplasmic flagella influence the shape of the entire cell even when not rotating. Inhibition of periplasmic flagellar rotation would result in cells that still retain their flat wave morphology. In support of this hypothesis, *B. burgdorferi* cells held at low temperature become nonmotile, but still retain their characteristic shape (4). To further test whether flagellar rotation is not necessary for the flat-wave morphology, cells were treated with the hydrogen ion uncoupler CCCP. This agent has been shown to rapidly cause immobilization and inhibition of flagellar rotation in bacteria that use the proton gradient for flagellar rotation (25, 32). We found that CCCP-treated cells of wild-type *B. burgdorferi* were immobilized within 15 min. These results indicate that the hydrogen ion gradient is used for periplasmic flagellar rotation in *B. burgdorferi*. In addition, the paralyzed cells still retained their flat-wave morphology (not shown). Thus, rotation of the periplasmic flagella is not necessary to impart the flat-wave morphology found in intact cells.

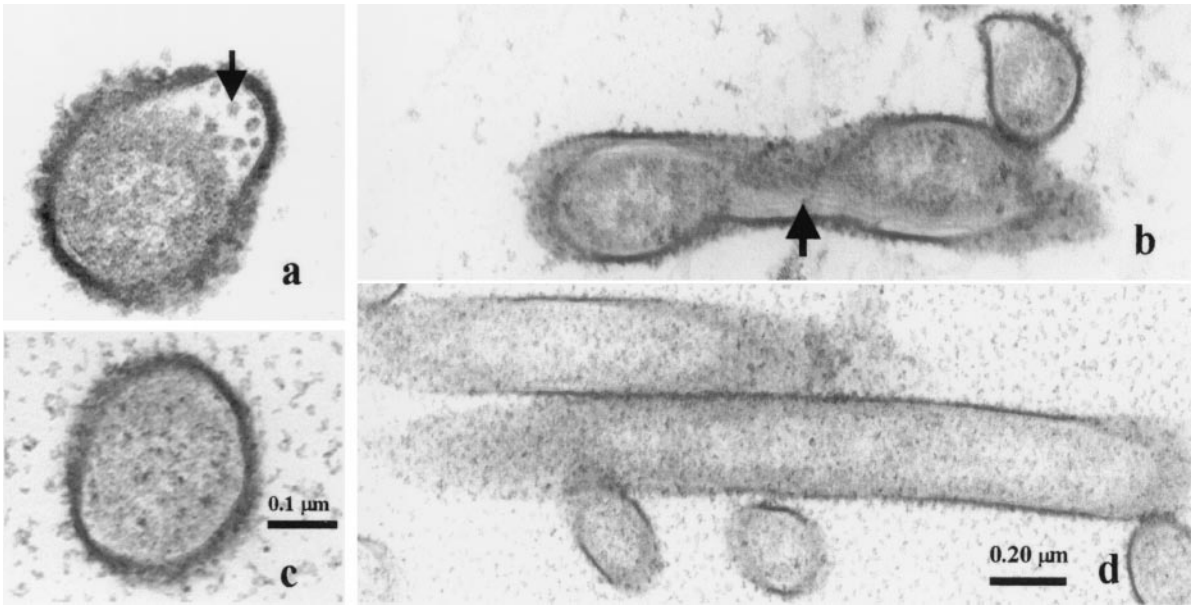

Fig. 4. Electron microscopic analysis of the wild-type (*a* and *b*) and mutant MC-1 (*c* and *d*). *a* and *c* represent cross sections, and *b* and *d* represent longitudinal sections. Arrows indicate periplasmic flagella.

Discussion

In the results reported here, the *flaB* mutant MC-1 was compared with the wild type. Because MC-1 retained its rod-shaped morphology and lack of motility even in the absence of kanamycin, we conclude that its altered phenotypes are the result of inactivation of the *flaB* gene, and not because of growth in kanamycin. In addition, several other kanamycin-resistant mutants with inserts in other genes had morphological shapes identical to the wild type (M.A.M., N.W.C., P.R., and D.S.S., unpublished observations). We emphasize the critical importance of drawing conclusions from the targeted mutation in *flaB* as opposed to the spontaneously occurring unmapped mutation (or mutations) in HB19Fla$^-$. For example, the HB19Fla$^-$ could conceivably have suffered a pleiotropic mutation (or mutations) in a regulatory gene that controls motility, periplasmic flagella synthesis, and morphology. Our results indicate that the *kan* insertion into *flaB* inhibits periplasmic flagella synthesis, resulting in a lack of motility and the altered cell morphology. Because *flaB* is monocistronically transcribed (18, 28), the altered phenotypes are not the result of downstream polar effects.

Factors determining bacterial cell shape are complex and varied. In most bacteria, cell morphology is determined by the peptidoglycan layer. For example, the determinants for whether a given bacterium is rod- or coccus-shaped reside within the structure of the murein sacculus (33, 34). Several enzymes and other proteins participate, with complex roles, in determining cell shape, and many of these proteins are associated with cell division (34). On the other hand, members of *Archaea*, which lack peptidoglycan, have other determinants that dictate cell morphology. For example, in some *Archaea*, cell shape is associated with the protein array S-layer (35). In other cases, such as the helically shaped *Spiroplasma* that also lacks peptidoglycan, the determinants of cell morphology are unknown (36).

The periplasmic flagella of spirochetes have been shown to influence cell morphology, but the results with *B. burgdorferi* are the most striking. In the *Leptospiracae*, several lines of evidence indicate that the short periplasmic flagella cause the ends of the cells to be either hook- or spiral-shaped (16, 30, 31, 37, 38). In *Treponema phagedenis*, which also has short periplasmic flagella, the presence of these organelles results in cells that have bent ends (39). The oral spirochete *T. denticola* has long periplasmic

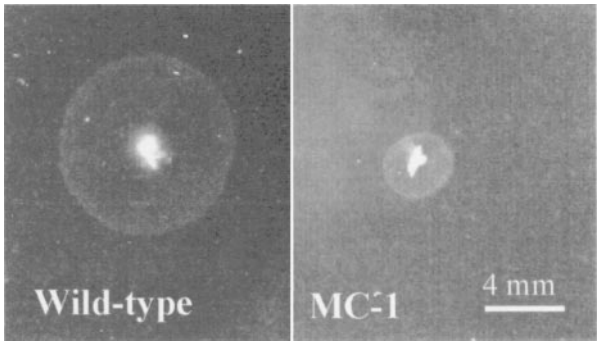

Fig. 5. Motility test using swarm agar plates. Swarm plates of mutant MC-1 and the wild type. Plates contained 0.35% agarose and were incubated for 4 days at 34°C.

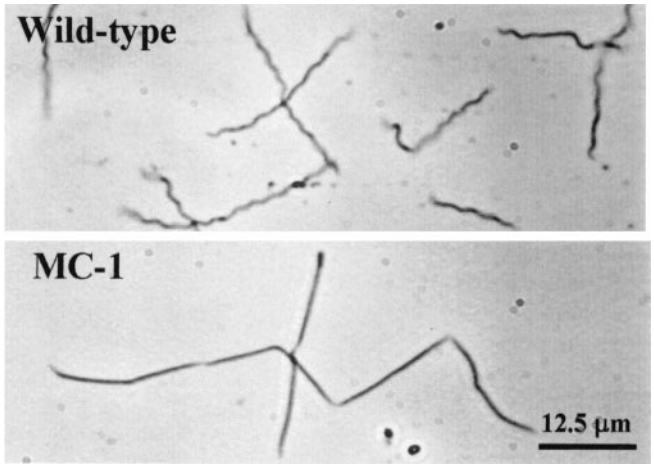

Fig. 6. Morphology of mutant MC-1 and the wild type as observed by phase microscopy.

flagella that overlap in the center of the cell. These spirochetes have both irregularly shaped and helically shaped motile cells. Because site-directed mutants lacking periplasmic flagella are not irregularly shaped but are helical, the periplasmic flagella are clearly associated with the irregular morphology (3). In all of these spirochete species, the cell body remains helical in mutants with either altered or deficient periplasmic flagella. In contrast, *B. burgdorferi flaB* mutants deficient in periplasmic flagella synthesis are rod-shaped.

Our results indicate that the morphology of *B. burgdorferi* is a function of two determinants. First, the peptidoglycan layer plays a primary role, as it determines the rod-shaped morphology of the cell cylinder. To support this contention, peptidoglycan has been shown to be a component of *B. burgdorferi* cell walls (40). In addition, cells with their outer membrane sheaths removed and treated with the peptidoglycan-degrading enzyme streptozyme readily lyse, which indicates that the peptidoglycan imparts rigidity to the cells in a manner similar to that of other bacteria (J. Kreiling and N.W.C., unpublished observations). Furthermore, *B. burgdorferi* is killed by both penicillin and vancomycin with accompanying cellular disruption (41). Future experiments whereby purified peptidoglycan is examined by electron microscopy should allow us to directly test whether this layer dictates the rod-shaped morphology. The secondary determinant of cell morphology, which is superimposed on the peptidoglycan layer, is the periplasmic flagella. Purified periplasmic flagella have been shown to be left-handed with a defined helix pitch (1.48 μm) and helix diameter (0.28 μm) (11); note that periplasmic flagella *in situ* as observed by high-voltage electron microscopy are also left-handed, but have a different helix pitch (2.83 μm) and helix diameter (0.40 μm) (16). Thus, two different interactions are important. First, the effect of the periplasmic flagella on the peptidoglycan is to confer the flat-wave morphology on the cell. Conversely, the effect of the peptidoglycan on the periplasmic flagella *in vivo* is to cause these organelles to deform to a shape with a different helix pitch and diameter than they have *in vitro*. We hypothesize that the structure integrating both of these interactions is the outer membrane sheath. This sheath juxtaposes both the peptidoglycan and the periplasmic flagella sufficiently close so that these structures can optimally interact with one another to promote cell motility.

The interaction of the periplasmic flagella with the peptidoglycan is complex. Bradfield and Cater (42) proposed in 1952 that the helical shape of some spirochetes is explained by the cell cylinder being a long rod, that a given periplasmic flagellum was attached at both ends, and that it wound around the cell. Contraction of these filaments caused the cells to be helically shaped (42). Although they were partially correct in that *B. burgdorferi* does indeed have a rod-shaped cell cylinder, their overall proposal was incorrect: a given periplasmic flagellum is attached to only one end (2, 5, 7, 43), and it rotates instead of contracts (4). Our finding that CCCP inhibits cell motility but does not alter the flat-wave morphology indicates that active energy transduction to the periplasmic flagella is not necessary for these organisms to retain their flat-wave morphology as suggested by their model. As an alternative proposal, Bradfield and Cater (42) also suggested that the periplasmic flagella have a real skeletal function, i.e., they function "as stiffeners." In this hypothesis, which they discounted as unlikely based on suggestive evidence they had at that time, they were correct.

The combination of efficient targeted mutagenesis methodology with complete genome sequence information is emerging as a powerful strategy to analyze gene function in *B. burgdorferi*. The recently proposed model of *B. burgdorferi* motility states that the periplasmic flagella rotate between the outer membrane sheath and cell cylinder, and that this rotation generates backward moving flat waves (4, 16, 19). In support of this model and as shown in this paper, FlaB and the periplasmic flagella were indeed found to be involved in cell shape and in motility. Future studies of mutants with mutations in some of the approximately 57 putative motility and chemotaxis genes identified from the genomic sequence should allow us to further test specific details of the model (13). For example, one aspect of the model proposes that in translating cells, the rotation of the periplasmic flagella bundles at both ends of the cell are coordinated, and that each bundle rotates in the opposite direction as viewed from the center of the cell (4, 16, 19). Accordingly, we predict the existence of certain genes that are involved in this coordination, and that disrupting these genes will lead to unusual phenotypes such as motile cells that translate very poorly and flex (i.e., bend in the center) more often than the wild type. Several of the genes that map within the motility gene clusters of *B. burgdorferi* have homologs in other spirochete species, but have no counterparts in other bacterial species (4, 13, 20, 21); conceivably, some of these genes could be involved in this coordination.

We thank C. Li, S. Goldstein, T. Elliott, M. Sal, and D. Yelton for helpful discussions and reviewing the manuscript, R. Macnab for strains, and A. Barbour for monoclonal antibodies. We appreciate the assistance of Diane Berry with electron microscopy. This research was supported by Public Health Service Grant AI29743.

1. Woese, C. R. (1987) *Microbiol. Rev.* **51,** 221–271.
2. Holt, S. C. (1978) *Microbiol. Rev.* **42,** 114–160.
3. Ruby, J. D., Li, H., Kuramitsu, H., Norris, S. J., Goldstein, S. F., Buttle, K. F. & Charon, N. W. (1997) *J. Bacteriol.* **179,** 1628–1635.
4. Goldstein, S. F., Charon, N. W. & Kreiling, J. A. (1994) *Proc. Natl. Acad. Sci. USA* **91,** 3433–3437.
5. Canale-Parola, E. (1984) in *Bergey's Manual of Systematic Bacteriology*, eds. Krieg, N. R. & Holt, J. G. (Williams & Wilkins, Baltimore), pp. 38–70.
6. Johnson, R. C. (1977) *Annu. Rev. Microbiol.* **31,** 89–106.
7. Barbour, A. G. & Hayes, S. F. (1986) *Microbiol. Rev.* **50,** 381–400.
8. Trott, D. J., Jensen, N. S., Saint Girons, I., Oxberry, S. L., Stanton, T. B., Lindquist, D. & Hampson, D. J. (1997) *J. Clin. Microbiol.* **35,** 482–485.
9. Li, H., Ruby, J., Charon, N. & Kuramitsu, H. (1996) *J. Bacteriol.* **178,** 3664–3667.
10. Limberger, R. J., Slivienski, L. L., Izard, J. & Samsonoff, W. A. (1999) *J. Bacteriol.* **181,** 3743–3750.
11. Charon, N. W., Goldstein, S. F., Block, S. M., Curci, K., Ruby, J. D., Kreiling, J. A. & Limberger, R. J. (1992) *J. Bacteriol.* **174,** 832–840.
12. Fraser, C. M., Norris, S. J., Weinstock, C. M., White, O., Sutton, G. G., Dodson, R., Gwinn, M., Hickey, E. K., Clayton, R., Ketchum, K. A., *et al.* (1998) *Science* **281,** 375–388.
13. Fraser, C. M., Casjens, S., Huang, W. M., Sutton, G. G., Clayton, R., Lathigra, R., White, O., Ketchum, K. A., Dodson, R., Hickey, E. K., *et al.* (1997) *Nature (London)* **390,** 580–586.
14. Ge, Y., Old, I. G., Saint Girons, I. & Charon, N. W. (1997) *J. Bacteriol.* **179,** 2289–2299.
15. Heinzerling, H. F., Olivares, M. & Burne, R. A. (1997) *Infect. Immun.* **65,** 2041–2051.
16. Goldstein, S. F., Buttle, K. F. & Charon, N. W. (1996) *J. Bacteriol.* **178,** 6539–6545.
17. Ge, Y., Li, C., Corum, L., Slaughter, C. A. & Charon, N. W. (1998) *J. Bacteriol.* **180,** 2418–2425.
18. Sadziene, A., Thomas, D. D., Bundoc, V. G., Holt, S. C. & Barbour, A. G. (1991) *J. Clin. Invest.* **88,** 82–92.
19. Li, C., Motaleb, M. A., Sal, M., Goldstein, S. F. & Charon, N. W. (2000) *J. Mol. Microbiol. Biotechnol.* **2,** 345–354.
20. Ge, Y., Old, I. G., Saint Girons, I. & Charon, N. W. (1997) *Microbiology* **143,** 1681–1690.
21. Ge, Y. G. & Charon, N. W. (1997) *Gene* **189,** 195–201.
22. Bono, J. L., Elias, A. F., Kupko, J. J., III, Stevenson, B., Tilly, K. & Rosa, P. (2000) *J. Bacteriol.* **182,** 2445–2452.
23. Samuels, D. S., Mach, K. E. & Garon, C. F. (1994) *J. Bacteriol.* **176,** 6045–6049.
24. Barbour, A. G. (1984) *Yale J. Biol. Med.* **57,** 521–525.
25. Goulbourne, E. A., Jr. & Greenberg, E. P. (1980) *J. Bacteriol.* **143,** 1450–1457.
26. Sambrook, J., Fritsch, E. F. & Maniatis, T. (1989) *Molecular Cloning: A Laboratory Manual* (Cold Spring Harbor Lab. Press, Plainview, NY), 2nd Ed.
27. Barbour, A. G., Hayes, S. F., Heiland, R. A., Schrumpf, M. E. & Tessier, S. L. (1986) *Infect. Immun.* **52,** 549–554.
28. Gassmann, G. S., Jacobs, E., Deutzmann, R. & Gobel, U. B. (1991) *J. Bacteriol.* **173,** 1452–1459.

29. Rosa, P., Samuels, D. S., Hogan, D., Stevenson, B., Casjens, S. & Tilly, K. (1996) *J. Bacteriol.* **178,** 5946–5953.
30. Berg, H. C., Bromley, D. B. & Charon, N. W. (1978) *Symp. Soc. Gen. Microbiol.* **28,** 285- 294.
31. Goldstein, S. F. & Charon, N. W. (1990) *Proc. Natl. Acad. Sci. USA* **87,** 4895–4899.
32. Shioi, J.-I., Matsuura, S. & Imae, Y. (1980) *J. Bacteriol.* **144,** 891–897.
33. Doyle, R. J. & Marquis, R. E. (1994) *Trends Microbiol.* **2,** 57–60.
34. Denome, S. A., Elf, P. K., Henderson, T. A., Nelson, D. E. & Young, K. D. (1999) *J. Bacteriol.* **181,** 3981–3993.
35. Beveridge, T. J., Pouwels, P. H., Sara, M., Kotiranta, A., Lounatmaa, K., Kari, K., Kerosuo, E., Haapasalo, M., Egelseer, E. M., Schocher, I., *et al.* (1997) *FEMS Microbiol. Rev.* **20,** 99–149.
36. Jacob, C., Nouzières, F., Duret, S., Bové, J. M. & Renaudin, J. (1997) *J. Bacteriol.* **179,** 4802–4810.
37. Bromley, D. B. & Charon, N. W. (1979) *J. Bacteriol.* **137,** 1406–1412.
38. Goldstein, S. F. & Charon, N. W. (1988) *Cell Motil. Cytoskel.* **9,** 101–110.
39. Charon, N. W., Goldstein, S. F., Curci, K. & Limberger, R. J. (1991) *J. Bacteriol.* **173,** 4820–4826.
40. Beck, G., Benach, J. L. & Habicht, G. S. (1990) *Biochem. Biophys. Res. Commun.* **167,** 89- 95.
41. Dever, L. L., Jorgensen, J. H. & Barbour, A. G. (1993) *Antimicrob. Agents Chemother.* **37,** 1115–1121.
42. Bradfield, J. R. G. & Cater, D. B. (1952) *Nature (London)* **169,** 944–946.
43. Hovind Hougen, K. (1984) *Yale J. Biol. Med.* **57,** 543–548.